Available online at www.sciencedirect.com
ScienceDirect
Atmospheric Environment 42 (2008) 1983–1994
ATMOSPHERIC ENVIRONMENT
www.elsevier.com/locate/atmosenv

Using environmental scanning electron microscopy to determine the hygroscopic properties of agricultural aerosols

Naruki Hiranuma[a,*], Sarah D. Brooks[a], Brent W. Auvermann[b], Rick Littleton[c]

[a]*Department of Atmospheric Sciences, Texas A&M University, 1204 Eller O&M Building, Mail Stop 3150, College Station, TX 77843, USA*
[b]*Texas A&M Research and Extension Center, 6500 Amarillo Blvd. West, Amarillo, TX 79106, USA*
[c]*The Microscopy and Imaging Center, Mail Stop 2257, Biological Sciences Building West, Texas A&M University, College Station, TX 77843-2257, USA*

Received 27 March 2007; received in revised form 12 September 2007; accepted 2 December 2007

Abstract

A field study at a cattle feedlot in the Texas Panhandle was conducted to characterize the hygroscopic, morphological, and chemical properties of agricultural aerosols and to identify possible correlations between these properties. To explore the hygroscopic nature of the agricultural particles, we have collected size-resolved aerosol samples using a cascade impactor system and have used an environmental scanning electron microscope (ESEM) to determine the water uptake by individual particles in those samples as a function of relative humidity (RH). In addition, complementary determination of the elemental composition of single particles was performed using energy dispersive X-ray spectroscopy (EDS). Our results indicate that most of the agricultural particles do not take up significant amounts of water when exposed to up to 96% RH. However, a small fraction of particles in the coarse mode deliquesced at approximately 75% RH and reached twice their original sizes by 96% RH. The observed changes in particle size with increased RH may significantly impact total aerosol extinction, visibility, and human health.

Keywords: Agricultural aerosol; Visibility; Hygroscopicity; Environmental scanning electron microscope (ESEM); Energy dispersive X-ray spectroscope (EDS)

1. Introduction

Agricultural fugitive dust is a significant source of localized air pollution in the semi-arid southern Great Plains. More than 40% of the US beef cattle are fed and processed in the High Plains of Texas, New Mexico, Oklahoma, Kansas, and Colorado (Koziel et al., 2005). In the Texas Panhandle, feedlots are often as large as one square mile in size. Daily episodes of elevated fugitive dust emissions from the feedlots are routinely observed in conjunction with increased cattle activity in the late afternoons and early evenings (Razote et al., 2004). During these dusty conditions at the corral edge of feedlots, mass concentrations of total suspended particulate (TSP) may be as high as $\sim$35,000 $\mu g/m^3$ for short periods of time (<6 h) (Sweeten et al., 1998). Fugitive dust from open-air

*Corresponding author. Tel.: +1 979 458 0177; fax: +1 979 862 4466.
E-mail addresses: naruki10@tamu.edu (N. Hiranuma), sbrooks@ariel.met.tamu.edu (S.D. Brooks), b-auvermann@tamu.edu (B.W. Auvermann), rickl@mic.tamu.edu (R. Littleton).

1352-2310/$ - see front matter © 2007 Elsevier Ltd. All rights reserved.
doi:10.1016/j.atmosenv.2007.12.003

agricultural feeding operations reduces visibility and has deleterious environmental impacts on inhabitants of nearby towns (Auvermann et al., 2004). Due to significant atmospheric loadings of agricultural dust aerosols, these aerosols must be considered in assessments of the impacts of aerosols on visibility, climate forcing and human health.

Particle size, composition and refractive index all change as a particle grows and dilutes at increased relative humidities. These changes make accurate predictions of aerosol extinction coefficients difficult (Hand and Kreidenweis, 2002). Previously, we have made direct measurements of atmospheric extinction at a cattle feedlot and those measurements indicate significant decreases in visibility during fugitive dust events as well as a wide variability in the reductions (Hiranuma, 2005). In that study, simultaneous measurements of the atmospheric extinction coefficient and the mass concentrations of coarse particles were made using an open-path transmissometer and tapered element oscillating microbalances (TEOMs), respectively. Two TEOMs were installed, one with a TSP inlet and one with a size-selective inlet for particulate matters (PM) with aerodynamic equivalent diameters of 10 μm or less (PM_{10}). At relative humidities (RH) less than 40%, a strong correlation between aerosol extinction and particulate mass was found. However, at high relative humidities ($RH \geqslant 80\%$), the PM concentrations and extinction coefficient were poorly correlated, suggesting that some or all of the fugitive dust particles takes up water, resulting in increased size and changes in the optical properties of the particles. In addition to informing us of the water uptake capacity of fugitive dust particles, the hygroscopicity measurements presented here may lend context to the ongoing and future transmissometry measurements at cattle feedlots.

Previous hygroscopicity measurements have been conducted on numerous atmospherically relevant compounds and mixtures, including Chan and Chan (2003), Choi and Chan (2002a, b), Gysel et al. (2004), Hameri and Rood (1992), Hansson et al. (1998), Badger et al. (2006) and Brooks et al. (2002, 2003, 2004). A number of techniques have been used to reliably measure the hygroscopicity of fine aerosol particles, for example, FTIR spectroscopy (Brooks et al., 2004), electrodynamic balance (Tang and Munkelwitz, 1993) and tandem differential mobility analyzers, (Cruz and Pandis, 2000). The environmental scanning electron microscope (ESEM) technique employed here was previously used by Ebert et al. (2002) and Krueger et al. (2003). The ESEM has two specific advantages over other techniques, namely determination of the hygroscopic properties of a single particle and the advantage of studying aerosols in wide range of sizes (Ebert et al., 2002). While pertinent measurements of water uptake as a function of RH have been conducted on humic materials (Brooks et al., 2004), we are not aware of any similar studies specifically on agricultural dust particles.

Here we report measurements of the hygroscopicity of size-selected agricultural aerosols collected from a ground site at the nominal downwind and upwind edges of a feedlot in the Texas Panhandle. ESEM was used to acquire detailed images of agricultural particulates as a function of RH. The variations in hygroscopicity due to location in relation to the feedlot and time of day are discussed below. In addition, the energy dispersive X-ray spectroscope (EDS) was used to determine the elemental composition of single particles. Relationships between particle morphology and composition are also discussed.

2. Experimental methods

2.1. Aerosol sampling

In August 2005, we conducted a measurement campaign in Tulia, TX, in the Texas Panhandle, where 45,000 head of cattle are housed in an open-air feedlot (2.6 km^2), "Feedlot C". Feedlot C is a representative open air Texas Cattle Feeding Association (TCFA) operation. At all TCFA facilities including Feedlot C, certain procedures are routinely conducted to minimize dust emissions, including spraying water on the surface of the pens and removal of loose manure (Sweeten, 1979). Local weather conditions at Feedlot C include large diurnal variation in temperature and relative humidity (RH), with the RH peaking in the coolest hours in morning hours (Mitchell et al., 1974). Afternoons and evenings typically have cooler temperatures, lower relative humidities, and lower wind speeds, concurrent with increased cattle activity. Major dust events occur when dry, uncompacted manure accumulates on the feedlot surface and dust is suspended by hoof action of the active cattle (Razote et al., 2006).

A low-volume cascade impactor system from PIXE, Inc. was mounted in a protective instrument

housing ~2 m above the ground at a sampling site located at the center point along the northern edge of the feedlot. This is nominally the downwind side of the feedlot. A number of complimentary measurements were underway at Feedlot C during this time, as described in Hiranuma (2005). Cascade impactor samples were also collected from a second site at the nominally upwind site of the lot. The cascade impactors were used to collect six size-resolved samples on aluminum foil filters in the sizes of <0.5, 0.5–1, 1–2, 2–8, 8–16 and $>16\,\mu m$. Using the electron microscope, we later observed that a number of particles on the filters were outside the specified size ranges. Several factors including turbulence, inconsistent flow rate, and irregular shape and density of agricultural dust may have contributed to the lack of distinct size cut-off points in the cascade impactor sampling (Kavouras and Koutrakis, 2001). Thus, we consider the cascade impactors sizing to be an initial sorting of the particle size. Using the electron microscope, all particles were grouped in three size ranges (>10, 2.5–10 and $<2.5\,\mu m$ diameter). Particles were further sorted by their shape as described in the next section.

A total of 54 size-selected filter samples were collected during three sampling periods in the morning, afternoon, and evening, from approximately 5:00–8:00, 15:00–18:00, 20:00–23:00 central daylight time (CDT), respectively, on 7, 8 and 11 August 2005. The samples collected on 7 and 8 August were collected on the nominally downwind side of the feedlot, and the August 11th samples were collected on the nominally upwind side for comparison. A sampling time of approximately 3 h was used for each sample. We consider the particles collected on these days to be representative of agricultural particles present in the summer in the Texas Panhandle. Relatively high levels of dust over the feedlot were visually observed on these days. Wind directions were southerly on all three days. During the collection periods, the TEOM measured 1-min peak concentrations as high as $\sim 8300\,\mu g\,m^{-3}$ on 11 August.

All samples collected in the field were transported in a refrigerated cooler to Texas A&M University and stored under refrigeration until microscopy analysis could be completed at the on-campus Microscope and Imaging Center. Water uptake measurements were conducted on a total of 169 individual particles collected with the cascade impactors.

2.2. ESEM measurements

Unlike standard electron microscopes which require vacuum conditions, the ESEM used in this study can be operated at higher pressures which allow the operator to introduce controlled amounts of gases, such as water vapor, to the sampling chamber. Here, the ESEM was used for two purposes. First, high-resolution images of the collected particles were obtained, allowing us to qualitatively describe the shape and morphology of particles collected at the feedlot. Second, the ESEM was used to image particles to determine the hygroscopicity of particles by collecting a series of images at a controlled temperature while the RH was incrementally increased.

2.2.1. Morphology

We now describe the morphology of particles in each size range collected at the feedlot and imaged with the ESEM. From each size-selected filter sample, ESEM measurements were conducted on a number of individual particles. As expected, using the low-volume cascade impactors chosen for this study resulted in filter samples sparsely covered with particles which allowed us to probe individual particle characteristics. We focused our ESEM measurements on individual particles which were not in contact with any others. High-resolution images of submicron particles were obtained by introducing and controlling the amount of water vapor in the Electro Scan Model E-3 ESEM equipped with a temperature- controlled sample stage.

Upon initial inspection of the dry particle images obtained with the ESEM, we observed several distinct particle shapes recurring on filter samples of all sizes. Nearly all particles in all sizes can be broadly classified by one of three distinct shapes as follows: (A) smooth, rounded particles, (B) rough-surfaced, amorphous single particles, or (C) agglomerations of multiple amorphous particles. Representative images of particles of these types, referred to here as Types A, B, and C, respectively, are shown in Fig. 1. Of all the particles randomly selected and imaged, the majority of particles were classified as Type B (roughly 82%) while significantly fewer were identified as Type A (~7%) and Type C (~11%). At smaller sizes (less than 2.5 μm diameter), the population was weighted most heavily toward the rough-textured Type B particles.

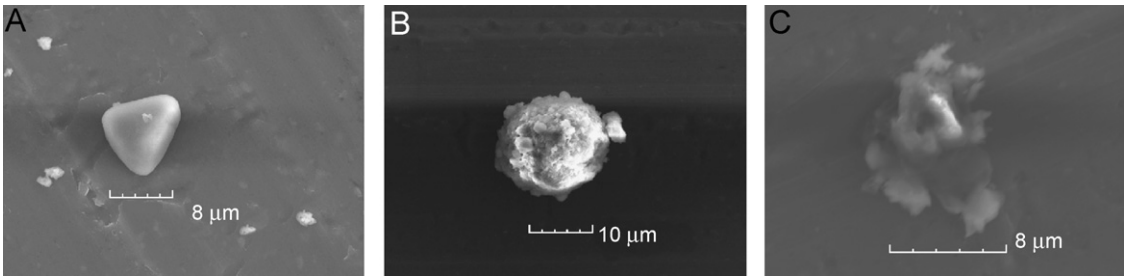

Fig. 1. Images of representative particles of the three types of particles observed: Types A, B and C are shown in 1A, 1B, and 1C, respectively.

This is the case for the samples collected at both the downwind and upwind sampling sites.

Due to the consistent recurrence of particles which fit into these three distinct categories, we chose to conduct our hygroscopic measurements on particles in each shape group to determine whether morphology could be used as an indication of composition and thereby hygroscopic properties. Some compounds, specifically salts, do not take up water until a characteristic RH, the deliquescence relative humidity (DRH) is reached. At the DRH, aerosol particles spontaneously take up water to become solution droplets. To test our capability of using ESEM for water uptake studies, we first used the ESEM to determine the DRH of salts with well-characterized DRHs, including sodium chloride, ammonium sulfate, and sodium sulfate. The average diameter of the salt particles used in this study was ~20 μm.

2.2.2. *Hygroscopicity*

Experiments were conducted at a temperature of 15 °C. We chose to conduct our measurements at 15 °C since stability and accuracy in temperature, RH, and imaging are optimized at this temperature. At this temperature, the pressure in the sample chamber can be changed by small increments of 0.1 torr corresponding to a small RH changes of 0.7–0.8%. Samples are initially held for half an hour in the ESEM chamber at 2.5% RH to insure that the particles are initially dry. Next, the RH is incrementally increased by introducing a controlled amount of water vapor to the ESEM observation cell and waiting 1–3 min at a constant temperature of 15 °C prior to collecting an image. The RH was incrementally increased from 7.9% to 96% in each experiment. In a typical experiment, the total number of RH steps is 50. Smaller increases in RH step (0.7–0.8%) was used above 64% to identify the water uptake behavior and deliquescent RH as accurately as possible. We cannot collect satisfactory ESEM images below 7.9% RH, because the amount of water vapor is not sufficient enough to carry backscattered electrons to the ESEM detector. While conducting measurements above 96% RH would be useful, it is not possible using this technique since pressure and temperature in the sample chamber become unstable and difficult to control at relative humidities above this point.

Here we define the DRH as the point at which the change in hygroscopic growth factor, D/D_0, is largest over an incremental change in RH. For each type of salt particle, six to nine experiments were conducted. The water uptake behavior for NaCl crystals with dry diameters of ~20 μm, and for a ~10 μm diameter fugitive dust particles are shown in Fig. 2A and B, respectively. For the sodium chloride, no abrupt water uptake was observed at RH < 73% (Fig. 2A III). Spontaneous water uptake and droplet formation were observed immediately after the RH was increased from 73% to 74% (Fig. 2A IV). In contrast, it can be seen that the agricultural particle does not exhibit a distinct deliquescence point, but rather exhibits small increases in size as water is gradually taken up over the range of RHs shown here.

The increases in particle diameter as a function of RH are typically represented by plotting the hygroscopic growth factor, D/D_0, defined as the ratio of the particle's diameter at a certain RH by the initial dry particle diameter. In Fig. 3, D/D_0 is shown for each of the salts in this study. The y-axis error bars indicate the standard error in our measurements. The x-axis error bars represent experimental uncertainty in the RH measurements, as described below.

The RH in the ESEM chamber can be altered in a controllable fashion by incrementally increasing or decreasing the pressure in the chamber and directly cooling or heating the sample stage. This is

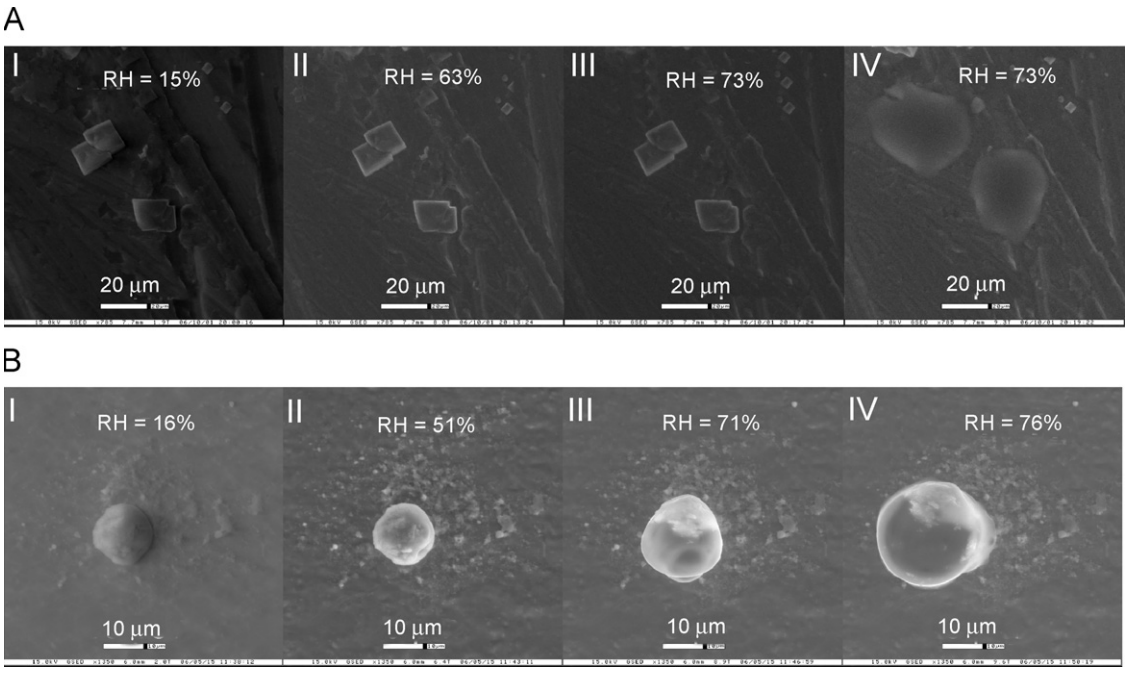

Fig. 2. ESEM images obtained during water uptake experiments. Particles in 2A are sodium chloride crystals (~20 μm diameter), and in 2B are from an agricultural sample (~10 μm diameter).

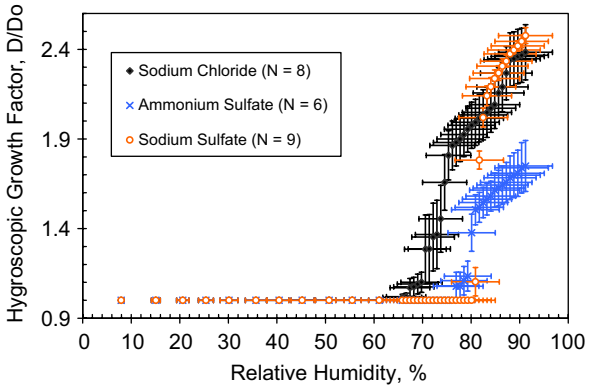

Fig. 3. Hygroscopic growth factor as a function of relative humidity for sodium chloride, ammonium sulfate and sodium sulfate is shown as solid diamonds, crosses, and open circle, respectively.

described by the Clausius–Clapeyron equation in the form shown below:

$$\mathrm{RH}(T) = \frac{P}{P_s \times \exp\left(\frac{L_v}{R_v} \times \left(\frac{1}{273} - \frac{1}{T}\right)\right)},$$

where RH(T) is the RH at given temperature (%), P the vapor pressure in the ESEM chamber (torr), P_s the saturation vapor pressure at 273 K (= 4.58 torr), L_v the latent heat of vaporization of water at 273 K (2.5×10^6 J K kg^{-1}), R_v the gas constant (461.5 J kg^{-1}).

Thus, the experimental uncertainties associated with the DRH measurements can be calculated using accuracy of pressure control unit and cooling stage. To calculate uncertainty involved in the RH measurement, we first converted all instrumental uncertainties to percent relative uncertainties. Instrumental accuracy of pressure control unit is within ±0.01 torr at given pressure, and calibration accuracy of temperature controller is computed as ±0.91 °C (CN9000A series operator's manual). We controlled the RH inside the ESEM chamber by altering pressure (i.e., amount of water vapor) at constant temperature (15 °C) in all experiments so that uncertainties in the pressure measurement vary with pressure (±0.08–1%) whereas percent relative uncertainties in temperature measurement are uniform throughout the experiment (±6.08%). Then, we calculated the error of RH as follows:

$$\%\mathrm{error}[\mathrm{RH}] = \sqrt{(\%\mathrm{error}[P])^2 + (\%\mathrm{error}[T])^2}.$$

Finally, absolute uncertainty in RH is found by multiplying the magnitude of the reported RH by relative uncertainty. Thus, uncertainty in our measurements ranges from ±0.48% to 5.72% RH.

As can be seen in the figure, ammonium sulfate particles do not appreciably change in size until a RH of ~79%. Upon reaching 79%, they deliquesce and abruptly increase in size. A sharp deliquescence point is also observed in the sodium sulfate data at ~82% RH. In the case of the sodium chloride, a small amount of water is taken up at 68% RH, indicating the onset of deliquescence with full deliquescence occurring by ~72% RH. This slight range in relative humidities may be an indication that the NaCl used contained an impurity of some kind. Our initial experiments were conducted on sodium chloride obtained from Sigma-Aldrich of $\geqslant$99.0% grade purity. To check for possible contamination, we repeated the NaCl experiments with NaCl from another source (Fluka, $\geqslant$99.5% grade purity). Once again, water uptake was observed over a small range of relative humidities. Nevertheless, our overall results for these salts are in good agreement with previous measurements, as we now discuss.

One complication is that the previous deliquescence studies which we wish to compare were conducted at 25 °C. Since deliquescence is a function of temperature, a direct comparison cannot be made. However, fortunately, a method has been developed by Tang and Munkelwitz (1993) to predict DRH as a function of temperature, provided that the DRH has been determined at one temperature. Using the equation below, we calculate the expected DRH at 25 °C based on our measurements at 15 °C.

$$\mathrm{DRH}(298) = \frac{\mathrm{DRH}(T)}{\exp\left\{\dfrac{\Delta H_s \times \left[A \times \left(\dfrac{1}{T} - \dfrac{1}{298}\right) - B \times \ln\left(\dfrac{T}{298}\right) - C \times (T - 298)\right]}{R}\right\}},$$

where DRH(T) is the deliquescence relative humidity at temperature T (in Kelvin), R the universal gas constant = 1.99 cal mol^{-1} K^{-1}, ΔH_s the enthalpy of solution, A, B, C the empirical constants.

The enthalpy values (ΔHs) used here, 448, 1510, and −2330 cal mol^{-1} for NaCl, $(NH_4)_2SO_4$, and Na_2SO_4, respectively, were calculated using data from a standard thermodynamic table in Wagman et al. (1965, 1982) and were assumed to be independent of temperature. Values for A, B and C, are taken from Tang and Munkelwitz (1993) and collectively represent the relationship between solubility and temperature.

We can now compare our predicted values of DRH at 25 °C to those of previous measurements obtained by others using ESEM and other techniques. This comparison is shown in detail in Fig. 4. Again, our predictions for DRH at 25 °C are based on the deliquescence measurements at 15 °C.

As can be seen from Fig. 4, the predicted DRH obtained by ESEM agree within our experimental error to results measured with other techniques. However for each salt studied, we observed deliquescence at a slightly lower RH than reported by others using a variety of experimental techniques including ESEM. Possible reasons for this offset of ~3% RH include uncertainty in the temperature measurement, uncertainty of the water vapor pressure measurement, and the standard deviation in our measurements. Another possibility is that the ESEM has the advantage of a longer equilibration time (1–3 min) for each set of new conditions than is possible for most of the other techniques (Ebert et al., 2002). To further confirm that particles have had adequate time to equilibrate at each RH, we conducted a time interval test. ESEM water uptake experiments were conducted on Na_2SO_4 particles. In this study, at each successive RH, the hygroscopic growth factor was measured at 1, 3, 5, and 10 min. The results showed no significant differences between hygroscopic growth factor collected at each time interval for a given RH, up to 96% RH. Overall, we concluded that within our stated uncertainty, this technique is a reliable way to accurately determine the hygroscopic properties of aerosol particles and one of the techniques that has a capability of obtaining such data for single particles and for particles of the large sizes of interest in this study. In the Results section below, ESEM measurements on a total of 169 particles collected at the feedlot are presented and discussed.

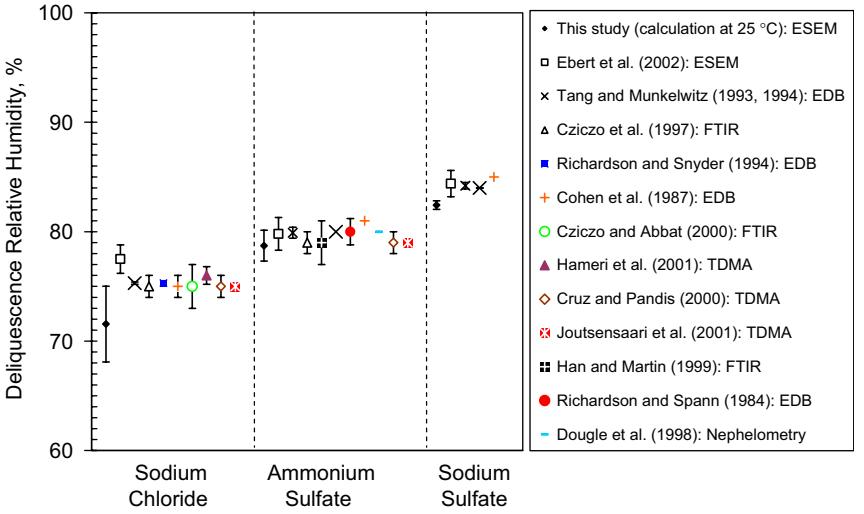

Fig. 4. Summary of the deliquescent relative humidities of well known salts by various techniques.

Attempts to determine the efflorescence RH, or RH at which aerosol particles lose water and recrystallize, were unsuccessful. Possible causes include heterogeneous nucleation on the substrate, compaction of projection area after the cycle of hydration and dehydration, and alteration of original shape during the deliquescence/efflorescence process observed in this study (Ebert et al., 2002; Köllensberger et al., 1999). Other techniques in which the aerosol is suspended, rather than in contact with a substrate, have had more success in measuring efflorescence (Dougle et al., 1998).

2.3. Elemental composition of agricultural aerosols

We conducted EDS measurements to identify the elemental composition of the particles in the three shape groups described above. A total of 208 particles collected at the feedlot were analyzed by EDS. In EDS, the X-ray detector measures the number of emitted X-rays as a function of their energy. Since elements have a characteristic energy, the EDS spectrum can be used to identify the quantity of elements present (Frankel and Aitken, 1970). One advantage of the EDS technique is that the measurements of weight percentage for specified elements can be obtained on a single particle basis. Though it would be ideal to collect hygroscopicity and chemical information on the exactly same particles, it is not feasible because the ESEM and EDS are not available to us in a single microscope apparatus. Using a JEOL® JSM-6400 EDS with an energy dispersive X-ray detector, the 47 mm diameter cascade impactor samples were mounted on electron microprobe stubs. The following optimal operating conditions were used: a working distance of 15 mm, an electron accelerating voltage of 15 keV, a beam current of 1 nA, and an analysis time greater than 60 s. To minimize background noise, we employed high magnifications, specifically 3×10^5 times for the particles that have diameters of smaller than 2.5 μm and 1.5×10^5 times for the particles that are larger than 2.5 μm in diameter.

3. Results and discussion

3.1. Hygroscopicity of fugitive dust particles and relation with morphology

Having shown that the ESEM technique can be accurately used to determine the hygroscopic behavior of aerosols, we report our results on agricultural dust particles. Water uptake studies were conducted on agricultural particles in three size ranges (>10, 2.5–10 and <2.5 μm diameter). Within each size range, experiments were conducted on particles in each shape group observed above (Types A, B and C). The hygroscopic growth factor (D/D_o) and DRH of 87 individual agricultural particles from downwind samples were determined using ESEM at a temperature of 15 °C. Water uptake as a function of RH is plotted in Fig. 5.

A fraction of the coarse-mode particle population deliquesced at approximately 80% RH and grew to twice of their original dry sizes at an RH of 96%. As can be seen from Fig. 5A and B, distinct

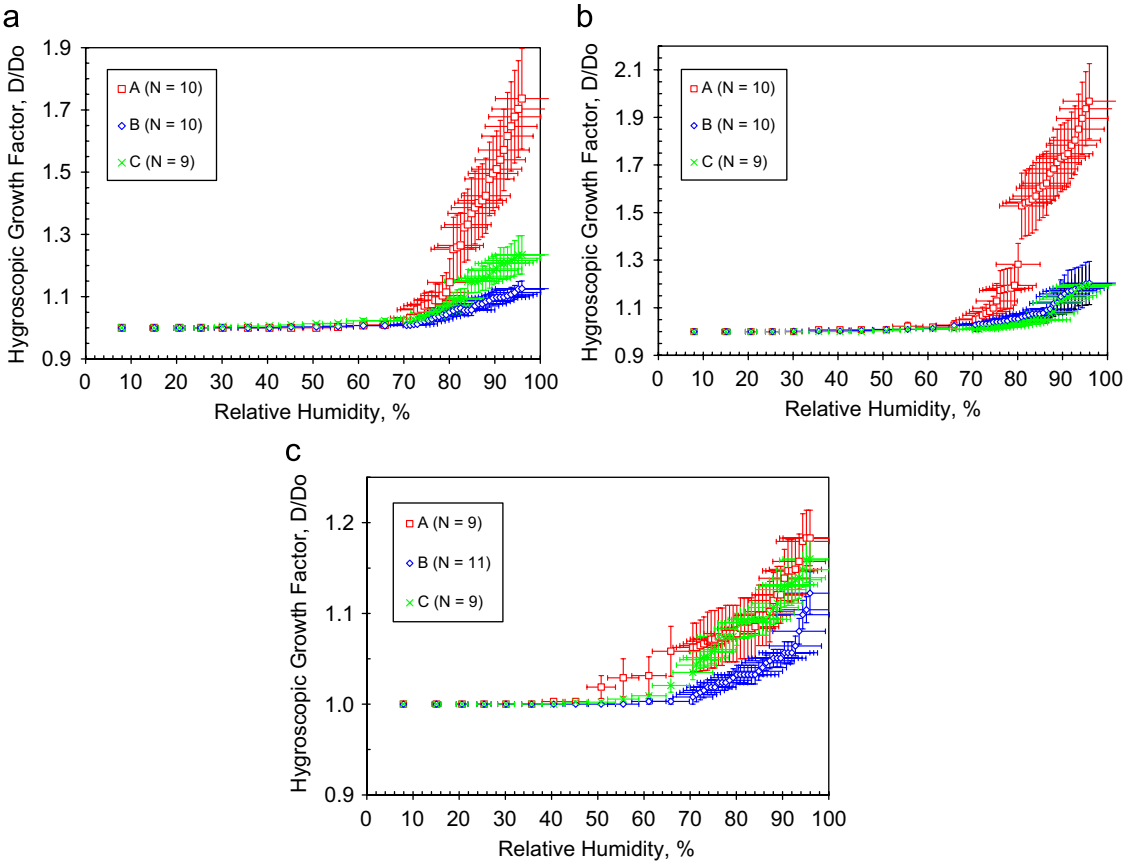

Fig. 5. Hygroscopic growth factor as a function of relative humidity for particles collected at the downwind edge of the feedlot in size range >1, 2.5–10 μm, and <2.5 μm are shown 5A, 5B, and 5C, respectively.

deliquescence behavior was observed only for the smooth rounded particles (Type A) that have dry diameters (D_o) larger than 2.5 μm. The DRH of these agricultural aerosols were determined as $79.5 \pm 7.0\%$ for particles that have D_0 of >10 μm and $76.3 \pm 9.5\%$ for particles that have D_0 of 2.5–10 μm. The hygroscopic growth factors calculated at 96% RH were 1.8 ± 0.4 and 2.0 ± 0.5 for the largest and intermediate size ranges, respectively. The maximum change in growth factor resulting from an increase a 0.1 torr increase in pressure (corresponding to a ~0.7% increase in RH) was 0.4 ± 0.3 for particles in both of these size ranges. The observed variability in DRH for individual particles indicates that the composition of agricultural particles is not uniform. The observed difference in hygroscopic growth factors for each size range suggests that particle size also has an influence on hygroscopicity. In the size range of <2.5 μm diameter, Type A particles took up only a small amount of water, starting at ~70% RH and gradually increasing up to 96% RH. In all size ranges, particles in the other shapes (Types B and C) gradually took up only a small amount of water uptake at and above 70% RH. In these cases, no abrupt change in water uptake or particle size was observed at any RH, indicating Types B and C particles do not contain significant concentrations of deliquescent materials.

To look for statistically significant trends in uptake behavior, we first attempted to identify several parameters which quantitatively describe a particle's water uptake behavior. The "hygroscopicity parameters" chosen were the DRH (for those samples with a clearly identifiable deliquescence point), the maximum increase in the hygroscopic growth factor due to an increase of ~0.7% RH, and the hygroscopic growth factor at 96% RH (the highest RH achieved in our ESEM experiments). All data collected were pooled into data subsets according to several factors: particle dry size, particle shape, sampling location, and sampling

time of day. A mean value was computed for each hygroscopicity parameter for each subset. These mean values were then compared to see if any of the data subsets were statistically unique at the 95% confidence limit (Hoshmand, 1988).

Based on this analysis, we can conclude that in the two larger sizes (>10 and 2.5–10 μm diameter) Type A particles took up a significant amount of water near 75–80% RH. This deliquescent behavior is statistically different (95% confidence) than the behavior of particles in the other two shape groups which took up only small amounts of water, even at high RH. For particles smaller than 2.5 μm, Type A particles took up only a small amount of water, starting at ~50% RH and gradually increasing above 50% RH. This behavior is similar to the behavior of particles in the other shapes (Types B and C).

DRH of 82 individual agricultural particles from upwind samples were determined using ESEM at a temperature of 15 °C. Particles collected at the upwind site took up slightly more water than those at the downwind site. While qualitatively the growth curves for particles on the downwind and upwind side of the feedlot were somewhat different, we observed that all hygroscopic parameters were statistically similar (within 95% confidence) for the nominally upwind and downwind sampling locations. This suggests that samples collected on the nominally upwind edge have similar compositions on these days, perhaps due to horizontal mixing of feedlot dust. Likewise, samples collected during morning, afternoon and evening all exhibited similar behavior (within 95% confidence), suggesting that no notable changes in composition occur throughout the day. This implies that changes in overall concentrations and changes in RH throughout the day may be responsible for changes in visibility as observed by the transmissometry measurements.

As shown in Fig. 6, we compared our results to the water uptake behavior of some common components of atmospheric aerosols, including ammonium sulfate and humic materials, in a further effort to identify the possible composition of the aerosols. For these purposes, ammonium sulfate was chosen as a representative of the major component of background sulfate aerosol. Humic materials (e.g., Pahokee Peat Reference humic acid and Suwannee River fulvic acid) were chosen due to a number of studies that suggest a large fraction of organic aerosol present in the atmosphere can be

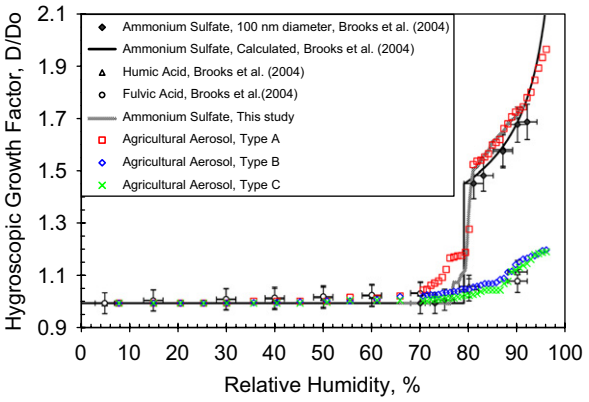

Fig. 6. Hygroscopic growth factor for particles collected during this study and known compositions: Agricultural aerosol data is for downwind in size range of 2.5–10 μm.

classified as humic materials and due to the likelihood that the agricultural dust would contain large amounts of decaying organic matter, such as humic-like materials (Ghio et al., 1996). Interestingly, the water uptake pattern exhibited by Type B and C is very similar to the behavior of particles containing the humic materials (Brooks et al., 2004) (Fig. 6). While we cannot say for certain, these data suggest that particles in Shape Groups B and C collected at the feedlot may contain significant fractions of soil or humic-like materials.

3.2. Elemental composition of fugitive dust particles and relation with morphology

EDS was used to determine the elemental composition of particles in three groups described above. In this study, particles in each size range (i.e., >10, 2.5–10 and <2.5 μm), 208 in total, were analyzed by EDS. The averaged relative weight percentage of each element was measured for particles in three different size ranges (i.e., >10, 2.5–10, and <2.5 μm) and the shape types (Types A, B, and C) in this study.

EDS measurements showed that particles of all types in this study are composed predominated of carbon. The carbon content is especially large in the non-hygroscopic particles (which included particles of Types B and C in the larger sizes and all three particle types in the <2.5 μm diameter range). The following 12 elements; C, N, O, Na, Mg, Si, P, S, Cl, Ar, K, and Ca were also detected in lower concentrations in particles of all types and sizes. Uncertainty in the reported percentages is within ±3–5% for each element studied. The high carbon

concentrations we observed were consistent with previous findings. For example, Rogge et al. (2006) stated that the organic matter content of fugitive dust emissions from concentrated cattle operations is mainly related to the original diet and chemical conversions in the digestive tracts of cattle. Weingartner et al. (1997) stated that the carbon particles are formed by aggregation, and some agglomeration occurs, forming branched chains which may lead to the irregular structure which we see recurring in Type C.

Analysis was performed to determine whether observed variations in the elemental compositions were statistically significant with respect to the morphological features. We compared the relative weight percentage of 12 elements (C, N, O, Na, Mg, Si, P, S, Cl, Ar, K, and Ca). On average, Type A particles in all sizes contained a higher weight percentage potassium ($19.0 \pm 13.2\%$) than the both the Types B and C particles. A possible source of the potassium may be the inorganic minerals additives included in to cattle diets (Buchanan et al., 1996). No significant differences between particles of Types B and C were determined in any of the three sizes. This is expected since Type C is likely composed of agglomerations of single Type B particles. Other than potassium, EDS analysis did not yield any other information on composition differences of particles in the different shape groups.

4. Conclusions

This study was conducted in an effort to characterize the morphological, hygroscopic, and chemical properties of agricultural aerosols and to attempt to identify any correlations between these properties. Size-selected aerosol sampling was conducted on a large cattle feedlot near Tulia, TX. We employed a cascade impactor aerosol sampler at both the downwind and upwind edges of Feedlot C.

In each of the size ranges (i.e., >10, 2.5–10, and $<2.5\,\mu m$), high resolution images of the particles were obtained with ESEM. The shapes of nearly all particles collected could be described as one of the three shape types: (A) smooth, rounded particles, (B) amorphous particles, or (C) agglomerations of multiple amorphous particles. Overall, the corresponding number percentage for each shape group were roughly 7% for Type A, 82% for B, and 11% for C.

The water uptake behavior of size-selected agricultural aerosol was observed by ESEM as a function of RH. In the size range of 2.5–10 μm diameter and $>10\,\mu m$ diameter, aerosols of Type A had deliquescence points of 75–80% and increased to hygroscopic growth factors of 2 at RH 96%, while particles in Type B and C exhibited low water uptake over the full range of relative humidities studied (up to 96% RH). At sizes less than $2.5\,\mu m$ diameter, particles of all shaped exhibited low water uptake.

We did not observe any statistically significant differences in hygroscopicity of particles collected at the nominally downwind and upwind edges of Feedlot C. Hygroscopic parameters considered in this analysis include the DRH (for those samples with a distinct deliquescence point), the maximum increase in the hygroscopic growth factor due to a 0.1 torr increase in pressure corresponding to a 0.7–0.8% increase in RH, and the hygroscopic growth factor at 96% RH (the highest RH achieved in our ESEM experiments). Likewise, samples collected during morning, afternoon and evening had similar hygroscopicity.

In addition, elemental analysis of the particles showed that the largest fraction of chemical composition of agricultural aerosols was carbon ($>75\%$). Also, Type A particles in the size range of $>10\,\mu m$ and 2.5–10 μm contain significant amount of potassium ($\sim 19\%$). This indicates that potassium may enhance the hygroscopicity of agricultural aerosols. Schönherr and Luber (2001) reported that salts of potassium deliquesce over a wide range of relative humidities (KCl 86%, K_2CO_3 44%, KNO_3 95%, and KH_2PO_4 97%). To further explore the relationship between hygroscopicity and chemical composition, future studies of chemical composition analysis are needed. For example, Raman microscopy can be used to obtain more detailed chemical information on a particle by particle basis.

Here we have observed that a percentage of the coarse agricultural particles readily take up water, while particles at the lower end of this range ($<2.5\,\mu m$) do not. Our results suggest that the changes in light scattering and visibility in the vicinity of cattle feedlots may be driven, in part, by water uptake and increased size of coarse particles as a function of changes in RH. Water uptake by the extremely high concentrations of coarse particles at the feedlot contributes to the increase in light attenuation and degradation of visibility causing the poor correlation between PM concentrations and extinction coefficient at high RHs ($RH \geqslant 80\%$). This is interesting since under most atmospheric

conditions, it is the fine, rather than coarse, particle fraction that drives changes in visibility. We do note one caveat of this study is that the water uptake measurements by ESEM cannot be performed on particles at very small sizes ($<1\,\mu m$). At low RH, measurements of total PM are strongly correlated with total extinction (Hiranuma, 2005). However, as one would expect based on the results presented here, at higher RH, this correlation is weaken. Further studies will include simultaneous measurements of mass concentration, extinction coefficient and hygroscopicity. The hygroscopicity data could be used to develop an RH-dependent correlation factor to account for changes in particle size and light scattering ability. RH-adjusted particulate mass concentrations could then be used as an accurate proxy for aerosol extinction over a broader range of RHs.

Acknowledgments

The authors would like to acknowledge the USDA CREES National Air Quality Initiative for funding this work, Grant no. 2006-35112-16636.

References

Auvermann, B.W., Hiranuma, N., Heflin, K., Marek, G.W., 2004. Open-path transmissometry for measurement of visibility impairment by fugitive emissions from livestock facilities. ASAE Conference Proceeding No. 044010. ASAE, Ottawa, Ontario, Canada.

Badger, C.L., Griffiths, P.T., George, I., Abbatt, J.P.D., Cox, R.A., 2006. Phase transitions and hygroscopic growth of aerosol particles containing humic acid and mixtures of humic acid and ammonium sulphate. Atmospheric Chemistry and Physics 6, 755–768.

Brooks, S.D., Wise, M.E., Cushing, M., Tolbert, M.A., 2002. Deliquescence behavior of organic/ammonium sulfate aerosol. Geophyiscal Research Letters 29 (19), 23.

Brooks, S.D., Garland, R.M., Wise, M.E., Prenni, A.J., Cushing, M., Hewitt, E., Tolbert, M.A., 2003. Phase changes in internally mixed maleic acid/ammonium sulfate aerosols. Journal of Geophysical Research 108 (D15), 21–23.

Brooks, S.D., DeMott, P.J., Kreidenweis, S.M., 2004. Water uptake by particles containing humic materials and mixtures of humic materials with ammonium sulfate. Atmospheric Environment 38, 1859–1868.

Buchanan, J.S., Berger, L.L., Ferrell, C., Fox, D.G., Galyean, M., Hutcheson, D.P., Klopfenstein, T.J., Spears, J., 1996. Nutrient Requirements of Beef Cattle: Subcommittee on Beef Cattle Nutrition, Committee on Animal Nutrition, Board on Agriculture, National Research Council. National Academy Press, Washington, DC.

Chan, M.N., Chan, C.K., 2003. Hygroscopic properties of two model humic-like substances and their mixtures with inorganics of atmospheric importance. Environmental Science and Technology 37 (22), 5109–5115.

Choi, M.Y., Chan, C.K., 2002a. Continuous measurements of the water activity of aqueous droplets of water-soluble organic compounds. Journal of Physical Chemistry A 106, 4566–4572.

Choi, M.Y., Chan, C.K., 2002b. The effects of organic species on the hygroscopic behaviors of inorganic aerosols. Environmental Science and Technology 36, 2422–2428.

Cruz, C.N., Pandis, S.D., 2000. Deliquescence and hygroscopic growth of mixed inorganic-organic atmospheric aerosol. Environmental Science and Technology 34, 4313–4319.

Dougle, P.G., Veefkind, J.P., ten Brink, H.M., 1998. Crystallization of mixtures of ammonium nitrate, ammonium sulphate and soot. Journal of Aerosol Science 29 (3), 375–386.

Ebert, M., Inerle-Hof, M., Weinbruch, S., 2002. Environmental scanning electron microscopy as a new technique to determine the hygroscopic behavior of individual aerosol particles. Atmospheric Environment 36, 5909–5916.

Frankel, R.S., Aitken, D.W., 1970. Energy dispersive X-ray emission spectroscopy. Applied Spectroscopy 24 (6), 557–566.

Ghio, A.J., Stonehuerner, J., Pritchard, R.J., Piantadosi, C.A., Quigley, D.R., Dreher, K.L., Costa, D.L., 1996. Humic-like substances in air pollution particulates correlate with concentrations of transition metals and oxidant generation. Inhalation Toxicology 8 (5), 479–494.

Gysel, M., Weingartner, E., Nyeki, S., Paulsen, D., Baltensperger, U., Galambos, I., Kiss, G., 2004. Hygroscopic properties of water-soluble matter and humic-likeorganics in atmospheric fine aerosol. Atmospheric Chemistry and Physics 4, 35–50.

Hameri, K., Rood, E.A.M., 1992. Hygroscopic properties of a NaCl aerosol coated with organic compounds. Journal of Aerosol Science 23, 437–440.

Hand, J.L., Kreidenweis, S.M., 2002. A new method for retrieving particle refractive index and effective density from aerosol size distribution data. Aerosol Science and Technology 36, 1012–1026.

Hansson, H.C., Rood, M.J., Koloutsou-Vakakis, S., Hameri, K., Orsini, D., Wiedensohler, A., 1998. NaCl aerosol particle hygroscopicity dependence on mixing with organic compounds. Journal of Atmospheric Chemistry 31 (3), 321–346.

Hiranuma, N., 2005. Open-path transmissometry to determine atmospheric extinction efficiency associated with feedyard dust. Thesis, West Texas A&M University, Canyon, TX.

Hoshmand, A.R., 1988. Statistical methods for environmental and agricultural sciences. CRC Press, Boca Raton, FL.

Kavouras, I.G., Koutrakis, P., 2001. Use of polyurethane foam as the impaction substrate/collection medium in conventional inertial impactors. Aerosol Science and Technology 34, 46–56.

Koziel, J.A., Parker, D.B., Baek, B-H., Bush, K.J., Mary, R., Perschbacher-Buser, Z., 2005. Ammonia and hydrogen sulfide flux from beef cattle pens: implications for air quality measurement methodologies and evaluation of emission controls. ASAE Conference Proceeding No. 701P0205. ASAE, St. Joseph, MI.

Köllensberger, G., Friedbacher, G., Kotzick, R., Niessner, R., Grasserbauer, M., 1999. In-situ atomic force microscopy investigation of aerosols exposed to different humidities. Fresenius Journal of Analytical Chemistry 364, 296–304.

Krueger, B.J., Grassian, V.H., Laskin, A., Cowin, J.P., 2003. The transformation of solid atmospheric particles into liquid droplets through heterogeneous chemistry: laboratory insights into

the processing of calcium containing mineral dust aerosol in the troposphere. Geophysical Research Letters 30, 48.

Mitchell, D.W., Jacquot, L.L., Chance, R.B., 1974. Soil Survey of Swisher County, Texas. United States Department of Agriculture, Soil Conservation Service in Cooperation with Texas Agricultural Experiment Station, Washington, DC.

Razote, E.B., Maghirang, R.G., Predicala, B.Z., Murphy, J.P., Auvermann, B.W., Harner, J.P., Hargrove, W.L., 2004. Dust-emission potential of cattle feedlots as affected by feedlot surface characteristics. ASAE Conference Proceeding No. 044015. ASAE, St. Joseph, MI.

Razote, E.B., Maghirang, R.G., Predicala, B.Z., Murphy, J.P., Auvermann, B.W., Harner, J.P., Hargrove, W.L., 2006. Laboratory evaluation of the dust-emission potential of cattle feedlot surfaces. Transactions of the ASAE 49 (4), 1117–1124.

Rogge, W.F., Medeiros, P.M., Simoneit, B.R.T., 2006. Organic maker compounds for surface soil and fugitive dust from open lot dairies and cattle feedlots. Atmospheric Environment 40, 27–49.

Schönherr, J., Luber, M., 2001. Cuticular penetration of potassium salts: effects of humidity, anions and temperature. Plant and Soil 236, 117–122.

Sweeten, J.M., 1979. Water works for dust control. Feedlot Management 20 (6), 28–31.

Sweeten, J.M., Parnell, C.B.J.R., Shaw, B.W., Auvermann, B.W., 1998. Particle size distribution of cattle feedlot dust emission. Transactions of the ASAE 41 (5), 1477–1481.

Tang, I.N., Munkelwitz, H.R., 1993. Composition and temperature dependence of the deliquescence properties of hygroscopic aerosols. Atmospheric Environment 27A, 467–473.

Wagman, D.D., et al., 1965. Selected Values of Thermodynamic Properties. National Bureau of Standards, Washington, DC.

Wagman, D.D., et al., 1982. The NBC tables of chemical thermodynamic properties. Journal of Physical and Chemical Reference Data 11 (Suppl. 2).

Weingartner, E., Burtescher, H., Baltensperger, U., 1997. Hygroscopic properties of carbon and diesel soot particles. Atmospheric Environment 31, 2311–2327.